Extremum Seeking Methods for Online Optimization of Spark Advance in Alternative Fueled Engines ⋆

Alireza Mohammadi * **Chris Manzie** * **Dragan Nešić** **

* *Department of Mechanical Engineering (e-mail: a.mohammadi@pgrad.unimelb.edu.au and manziec@unimelb.edu.au),*
** *Department of Electrical and Electronic Engineering (e-mail: dnesic@unimelb.edu.au), University of Melbourne, Parkville, 3010, Victoria, Australia.*

Abstract: Alternative fueled engines offer greater challenges for engine control courtesy of uncertain fuel composition. This make optimal tuning of input parameters like spark advance extremely difficult in most existing ECU architectures. This paper proposes the use of grey-box extremum seeking techniques to provide real-time optimization of the spark advance in alternative fueled engines. The ability and flexibility of the proposed framework is demonstrated through simulation examples. The approaches demonstrated may be extended to other engine inputs requiring online optimization.

Keywords: Engine control, Extremum seeking, Optimization, Parameter estimation, Alternative fuels.

1. INTRODUCTION

Nowadays, due to the increasingly demanding emissions legislation and growing concerns about the shortage of petroleum resources, the research and development into alternative fuels for automotive application has become an important subject. Alternative fuels such as ethanol and methanol mixture, LPG (Liquified Petroleum Gas), and CNG (Compressed Natural Gas) have lower fuel costs and cleaner exhaust gas emissions as compared with gasoline and diesel Kim et al. (2009). These fuels may also enhance energy security through increasing sources of reliable energy.

However, despite all of these advantages, the main drawback of these fuels is that their composition can vary depending on origination, season, and relative cost. The results of a study by Ly (2002) established significant variations between supply sources within large geographic areas such as Europe and Australia.

The change in composition of these fuels was found to have a profound effect on performance and emissions of alternative fueled engines, see Min et al. (1998). One reason is that current approaches to control of engines rely on static maps for steady-state operating points. In these methods, the optimum values of variables, such as spark timing and air/fuel ratio, are stored in a memory in engine control unit (ECU) for a finite number of engine operating set-points. The static maps must be robust enough to handle all possible fuel compositions, which implies detuning of closed-loop performance. Alternatively, the fuel composition must be sensed and calibration of the maps undertaken for all possible compositions. Consequently, the former approach results in suboptimal engine performance at any operating point, while latter involves more cost and calibration effort. Both are undesirable.

This points to the need for online adaption in order to optimize the engine performance as the mixture of fuel changes. Extremum seeking (ES) controllers typically provide online optimization in the presence of plant dynamics and slowly time-varying uncertainties. As a result, they warrant investigation as a potential solution to the fuel composition problem described above.

There are two main approaches for design of ES controllers. First there are methods which treat the system as a black-box, which for many applications means potentially disregarding known information about the model structure (Popovic et al. (2006), Killingsworth et al. (2009)). The second approach, which is used in this paper, incorporates a known plant structure with uncertain parameters in the online optimization of plant operation, referred to as grey-box ES controllers. In this latter approach, as shown in Fig. 1, the input of the plant is subjected to a perturbation and the resulting output perturbations are used to update estimates of the plant parameters. The updated parameter estimates are then used in an optimization scheme to update the input to the plant.

One of the early research works on grey-box ES in engine control has been used by Scotson and Wellstead (1990) to optimize the brake torque of a spark ignition engine as a function of the spark advance. Zarrop and Romments (1993) extended the results derived by Wellstead

⋆ This work was supported by Australia Research Council Discovery Grant, DP0985388.

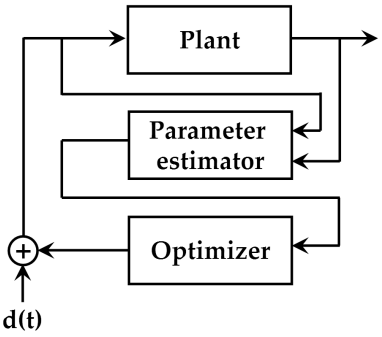

Fig. 1. General structure of grey-box extremum seeking control

and Scotson to the multi-input case. The lack of a rigorous convergence analysis in all of these attempts has limited the ability to guarantee much about the system performance. Egardt and Larsson (2005) used the same approach of Wellstead and Scotson for exactly the same application but they analyzed the role of probing in the control law and asymptotic properties of the grey-box ES controller. Nevertheless, their results are presented for particular classes of plants and particular optimization and estimation algorithms are used to achieve extremum seeking.

Nešić et al. (2013) proposed a general framework for design of grey-box ES controllers. This framework provides precise conditions under which a large class of continuous optimization algorithms can be combined with a large class of parameter estimators to achieve convergence of the closed loop trajectories to the desired extremum. This enables different combinations of parameter estimators and optimization algorithms without sacrificing the robustness of the closed-loop system. By comparing the performance of different combinations, the best online optimization approach from the combinations satisfying the assumptions of Nešić et al. (2013) can be determined. However, the results of Nešić et al. (2013) are presented in continuous-time while practical implementations of engine controllers are in discrete-time.

The first purpose of this paper is to take advantage of emulation design methods to introduce a discrete-time analog of the continuous-time ES framework proposed in Nešić et al. (2013). It is illustrated that under certain conditions the discretized controller preserves the closed-loop performance of the continuous-time controller under sampling.

The second objective of this study is to maximize the engine brake torque by finding the best spark advance using the proposed discrete-time ES framework in the presence of varying fuel composition. For this purpose, different combinations of estimation and optimization algorithms, satisfying required conditions of the framework, are used to locate the optimum spark advance corresponding to maximum brake torque (MBT) with unknown fuel composition.

2. THE FRAMEWORK FOR CONTINUOUS-TIME GREY-BOX ES CONTROLLER

In this section, first the grey-box ES framework for static plants is summarized from Nešić et al. (2013). Then, different estimation and optimization algorithms that satisfy conditions of the framework are provided and a particular combination of these algorithms is used to illustrate the verification of conditions of the framework.

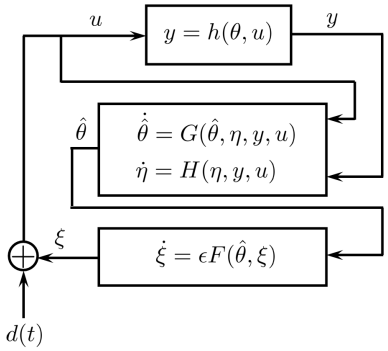

Fig. 2. The proposed framework for static plants

2.1 Notation

The set of real numbers is denoted by $\mathbb{R}$. The continuous function $\alpha : [0, a) \to \mathbb{R}_{\geq 0}$ is said to belong to class $\mathcal{K}$ if it is nondecreasing and $\alpha(0) = 0$. The continuous function $\beta : \mathbb{R}_{\geq 0} \times \mathbb{R}_{\geq 0} \to \mathbb{R}_{\geq 0}$ is a class of $\mathcal{KL}$ if it is nondecreasing in its first argument, strictly decreasing to zero in its second argument and $\beta(0, t) = 0$ for all $t \geq 0$. Let T denote the sampling period.

2.2 Grey-box ES Controller for Static Plants

Consider the following class of ES schemes, illustrated in Fig. 2:

$$y = h(\theta, u) \ , \tag{1}$$
$$u = \xi + d(t) \ , \tag{2}$$
$$\dot{\hat{\theta}} = G(\hat{\theta}, \eta, y, u) \ , \tag{3a}$$
$$\dot{\eta} = H(\eta, y, u) \ , \tag{3b}$$
$$\dot{\xi} = \epsilon \ F(\hat{\theta}, \xi) \ , \qquad \epsilon > 0 \tag{4}$$

where y is the output of the static plant model (1), θ is the vector of unknown parameters, and u is the input into the plant. In equation (2), $d(t)$ is a dither signal that is typically chosen so that appropriate parameter convergence can be achieved and ξ comes from the optimization algorithm (4). The optimization algorithm uses the estimated parameters $\hat{\theta}$ obtained from the parameter estimator (3a), (3b). The parameter estimation algorithm (3a) may contain extra states $\eta \in \mathbb{R}^q \times \mathbb{R}^s$ to widen the class of estimators considered. In optimization algorithm (4), ϵ is a controller tuning parameter (typically, a small positive number) that may be adjusted.

By introducing $\tilde{\theta} := \hat{\theta} - \theta$, $\tilde{\eta} := \eta - \eta^*$, $\tilde{\xi} := \xi - \xi^*$ (where (θ, η^*, ξ^*) is the equilibrium of (1)-(4)) and writing the closed loop equations in $\tilde{\theta}, \tilde{\eta}, \tilde{\xi}$ coordinates, the model of the systems (3a), (3b), (4) is obtained in the singular perturbation form:

$$\begin{aligned}\dot{\tilde{\theta}} &= G(\tilde{\theta}+\theta, \tilde{\eta}+\eta^*, h(\theta, \tilde{\xi}+\xi^*+d(t)), \\ &\quad \tilde{\xi}+\xi^*+d(t)) \\ &=: \widetilde{G}(t, \tilde{\theta}, \tilde{\eta}, \tilde{\xi}) \qquad (5a) \\ \dot{\tilde{\eta}} &= H(\tilde{\eta}+\eta^*, h(\theta, \tilde{\xi}+\xi^*+d(t)), \\ &\quad \tilde{\xi}+\xi^*+d(t)) \\ &=: \widetilde{H}(t, \tilde{\eta}, \tilde{\xi}) \qquad (5b) \\ \dot{\tilde{\xi}} &= \epsilon F(\tilde{\theta}+\theta, \tilde{\xi}+\xi^*) \\ &=: \epsilon \widetilde{F}(\tilde{\theta}, \tilde{\xi}) \qquad (6)\end{aligned}$$

Then, the following assumption guarantees that the continuous-time grey-box ES scheme (2)-(4) is stable and converges to optimum value of the static plant (1).

Assumption 1. The continuous-time closed-loop system (5a), (5b) and (6) is practically asymptotically stable, i.e., there exist $\beta_1, \beta_2, \beta_3 \in \mathcal{KL}$ and $\Delta > 0$ such that for any strictly positive real number $\nu > 0$, there exists $\epsilon^* > 0$ such that for all $\epsilon \in (0, \epsilon^*)$ the following holds:

$$|\tilde{\theta}(t)| \leq \beta_1(|(\tilde{\theta}(t_0), \tilde{\eta}(t_0), \tilde{\xi}(t_0))|, t-t_0) + \nu, \qquad (7)$$

$$|\tilde{\eta}(t)| \leq \beta_2(|(\tilde{\eta}(t_0), \tilde{\xi}(t_0))|, t-t_0) + \nu, \qquad (8)$$

$$|\tilde{\xi}(t)| \leq \beta_3\big(|\tilde{\xi}(t_0)|, \epsilon(t-t_0)\big) + \nu, \qquad (9)$$

for all $(\tilde{\theta}(t_0), \tilde{\eta}(t_0), \tilde{\xi}(t_0)) \in \mathcal{B}_\Delta \subset \Omega_{\tilde{\theta},\tilde{\eta}} \times \Omega_{\tilde{\xi}}$, and $t \geq t_0 \geq 0$. In particular, $\limsup_{t\to\infty} |\tilde{\theta}(t)| < \nu$, $\limsup_{t\to\infty} |\tilde{\eta}(t)| < \nu$ and $\limsup_{t\to\infty} |\tilde{\xi}(t)| < \nu$. □

Assumption 1 can be interpreted as follows. There exists a ball $\mathcal{B}_\Delta$ of initial conditions such that for any desired accuracy characterized by ν, the parameter ϵ can be adjusted so that for all initial conditions in the ball $\mathcal{B}_\Delta$:

- The parameter estimate $\hat{\theta}$ converges to the $\mathcal{B}_\nu$ ball centered at the true values of the parameters θ in time scale t (see (7));
- The extra state of the parameter estimator η converges to the $\mathcal{B}_\nu$ ball centered at the equilibrium of (3b) η^* in time scale t (see (8));
- The optimizer state ξ converges in the slow time scale ϵt to the $\mathcal{B}_\nu$ ball centered at the optimal value ξ^* (see (9)).

Sufficient conditions under which Assumption 1 holds are presented by Nešić et al. (2013).

2.3 Estimation Algorithms (EA)

In order to estimate the unknown parameters in (1) different type of parameter estimators in form of (3a), (3b) can be employed which satisfy required conditions of Assumption 1. Some examples from Ioannoua and Fidan (2006) and Baras et al. (1988) are:

- EA1. Gradient algorithm,
- EA2. Gradient algorithm with integral cost function,
- EA3. Pure least-squares algorithm,
- EA4. Recursive least-squares algorithm.

While all of these algorithms can be shown to satisfy Assumption 1, this is only demonstrated explicitly here for the recursive least-squares algorithm (EA4). For this purpose, a specific type of plant is required. So consider the following class of steady-state maps that are linearly parameterized with θ as

$$y = \phi^T(u)\theta. \qquad (10)$$

For this plant, the parameter update using EA4 is given by

$$\dot{\hat{\theta}} = -P\phi(u)(y - \phi(u)^T\hat{\theta}) := G(\hat{\theta}, y, u) \qquad (11a)$$

$$\dot{P} = \gamma P - P\phi(u)\phi(u)^T P := H(P, u) \qquad (11b)$$

where $\gamma \geq 0$ and P is the error covariance matrix. Using $u = \xi + d(t)$ and writing (11a) and (11b) in coordinates $\tilde{\theta} = \hat{\theta} - \theta$, $\tilde{P} = \hat{P} - P^*$ and $\tilde{\xi} = \xi - \xi^*$ gives:

$$\begin{aligned}\dot{\tilde{\theta}} &= -(\widetilde{P} + P^*)\phi\tilde{\theta} \\ &:= \widetilde{G}(\tilde{\theta}, \widetilde{P}, \tilde{\xi}) \qquad (12a) \\ \dot{\widetilde{P}} &= \gamma(\widetilde{P} + P^*) - (\widetilde{P} + P^*)\phi\phi^T(\widetilde{P} + P^*) \\ &:= \widetilde{H}(t, \widetilde{P}, \tilde{\xi}) \qquad (12b)\end{aligned}$$

According to (Nešić et al., 2013, Proposition 10), Assumption 1 holds for the estimator (12a), (12b) if $\phi(t)$ is persistently exciting, i.e., for all $t_0 \geq 0$ there exists $\mu, \sigma > 0$ such that

$$\int_{t_0}^{t_0+\sigma} \phi(\tau)\phi^T(\tau)d\tau \geq \mu I. \qquad (13)$$

By using an appropriate dither signal $d(t)$, $\phi(t)$ can be made persistently exciting.

In the next subsection optimization algorithms that can be combined with estimation algorithms in this subsection to satisfy Assumption 1 are provided.

2.4 Optimization Algorithms (OA)

Similar to the previous subsection, there exists a large class of optimization algorithms which satisfy the conditions of Assumption 1; some examples from Absil and Kurdyka (2006), Bhaya and Kaszkurewicz (2006), Zhang et al. (2008) and Tanabe (1985) are:

- OA1. Gradient descent algorithm,
- OA2. Continuous Newton method,
- OA3. Continuous Jacobian matrix transpose,
- OA4. Combination of Newton and gradient methods,
- OA5. Levenberg-Marquardt method,
- OA6. Newton-Raphson-Ben-Israel.

In order to demonstrate the verification of Assumption 1, the continuous Jacobian matrix transpose method (OA3) is chosen as the optimization algorithm:

$$\dot{\xi} = -\epsilon\Gamma J_r^T(\hat{\theta}, \xi)\nabla h(\hat{\theta}, \xi) \qquad (14)$$

$$:= \epsilon F(\hat{\theta}, \xi)\ , \qquad (15)$$

where $\nabla h(\xi)$ denotes the gradient of h at ξ, J_r represents the Jacobian of $r(\xi) = \nabla h(\xi)$ and Γ is an arbitrary positive definite matrix. Then, writing (15) in coordinates $\tilde{\theta} = \hat{\theta} - \theta$ and $\tilde{\xi} = \xi - \xi^*$ gives:

$$\begin{aligned}\dot{\tilde{\xi}} &= -\epsilon F(\tilde{\theta}+\theta, \tilde{\xi}+\xi) \\ &:= \widetilde{F}(\tilde{\theta}, \tilde{\xi}) \qquad (16)\end{aligned}$$

The above optimization algorithm, according to (Nešić et al., 2013, Proposition 3), satisfies Assumption 1 if the

Jacobian matrix $J_r(\xi)$ is invertible in some neighborhood of ξ^*.

Up to this point, the existing continuous-time grey-box ES framework and algorithms fitted to this framework are explained. In the next section, the discrete-time analog of this framework is investigated.

3. DISCRETE-TIME EMULATION DESIGN OF GREY-BOX ESC FRAMEWORK

In this section, first emulation design methods is explained for the general form of the plant, parameter estimator and optimization algorithm and the consequent main result is stated. Then, the main result is applied to the particular estimator and optimizer that explained in the previous section using a particular discretization method.

3.1 Emulation design of the grey-box framework

Emulation of a system consists of two steps: (1) the design of a continuous-time controller for a continuous-time plant using known continuous-time design methods to satisfy closed-loop control performance objectives, and (2) the discretization and implementation of the continuous-time controller using sample and hold devices as shown in Fig. 3, with the objective of obtaining comparable closed-loop system properties Pierre et al. (1995). The exact discretization of the parameter estimator (5a), (5b) and optimization algorithm (6) is obtained as

$$\begin{aligned}\tilde{\theta}^e(k+1) &= \tilde{\theta}^e(k) + \int_{kT}^{(k+1)T} \widetilde{G}(\tau, \tilde{\theta}(\tau), \tilde{\eta}(\tau), \tilde{\xi}(k))d\tau \\ &=: \widetilde{G}^e_T(k, \tilde{\theta}(k), \tilde{\eta}(k), \tilde{\xi}(k)) \qquad (17a)\\ \tilde{\eta}^e(k+1) &= \tilde{\eta}^e(k) + \int_{kT}^{(k+1)T} \widetilde{H}(\tau, \tilde{\eta}(\tau), \tilde{\xi}(k))d\tau \\ &=: \widetilde{H}^e_T(k, \tilde{\eta}(k), \tilde{\xi}(k)) \qquad (17b)\\ \tilde{\xi}^e(k+1) &= \tilde{\xi}^e(k) + \int_{kT}^{(k+1)T} \epsilon\widetilde{F}(\tilde{\theta}(k), \tilde{\xi}(\tau))d\tau \\ &=: \widetilde{F}^e_T(\tilde{\theta}(k), \tilde{\xi}(k), \epsilon) \qquad (18)\end{aligned}$$

where $\tilde{\theta}^e$, $\tilde{\eta}^e$ and $\tilde{\xi}^e$ are exact discrete values of the continuous-time states $\tilde{\theta}$, $\tilde{\eta}$ and $\tilde{\xi}$.

Due to the introduction of the new tuning parameter T and also due to the fact that, in general, it is impossible to compute $\widetilde{G}^e_T$ and $\widetilde{F}^e_T$ exactly, so instead an approximate discrete-time model of the controller should be used:

$$\tilde{\theta}^a(k+1) = \widetilde{G}^a_T(k, \tilde{\theta}(k), \tilde{\eta}(k), \tilde{\xi}(k)) \qquad (19a)$$

$$\tilde{\eta}^a(k+1) = \widetilde{H}^a_T(k, \tilde{\eta}(k), \tilde{\xi}(k)) \qquad (19b)$$

$$\tilde{\xi}^a(k+1) = \widetilde{F}^a_T(\tilde{\theta}(k), \tilde{\xi}(k), \epsilon) \qquad (20)$$

which are obtained from (5a), (5b) and (6) using one of the numerical integration methods (e.g. Runge-Kutta) and $\tilde{\theta}^a$, $\tilde{\eta}^a$ and $\tilde{\xi}^a$ are approximate discrete-time values of the continuous-time states $\tilde{\theta}$, $\tilde{\eta}$ and $\tilde{\xi}$.

In order to guarantee that the mismatch between the exact discrete-time model of the grey-box ES controller (17a), (17b) and (18) and its approximation (19a), (19b) and (20) is small, the conditions of Assumption 1 are not enough

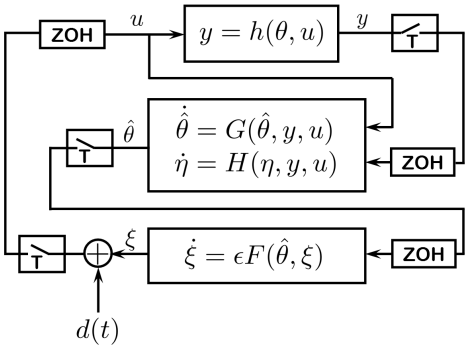

Fig. 3. Sample and zero order hold devices in the grey-box ES framework

and some form of consistency should be be considered. To this end, first one-step consistency is defined for a general nonlinear continuous-time system $\dot{\psi}(t) = \Psi(\psi(t))$ and its exact and approximate discretization as $\psi^e(k+1) = \Psi^e_T(\psi^e(k))$ and $\psi^a(k+1) = \Psi^a_T(\psi^a(k))$, respectively. Then, the required condition is stated based on the consistency definition.

Definition 1. $\Psi^a(\psi^a(k))$ is one-step consistent with $\Psi^e(\psi^e(k))$ if there exist Δ such that for any $|\psi| < \Delta$, there exists T^* such that for all $T \in (0, T^*)$ the following holds:

(1) Ψ^a_T is one-step consistent with $\Psi^{Euler}_T := \psi + T\Psi$, i.e., there exists a function $\rho \in \mathcal{K}_\infty$ such that:
$$|\Psi^a_T - \Psi^{Euler}_T| \leq T\rho(T)$$
(2) there exist $M > 0$ and $\gamma \in \mathcal{K}_\infty$ such that for all $|\psi| < \Delta$ and $|\zeta| < \Delta$:
- $|\Psi(\zeta)| \leq M$
- $|\Psi(\zeta) - \Psi(\psi)| \leq \gamma(|\zeta - \psi|)$. □

Now the following assumption is considered for the exact and approximate discretization of the estimation and optimization algorithms.

Assumption 2. $\widetilde{G}^a_T(k, \tilde{\theta}, \tilde{\eta}, \tilde{\xi})$, $\widetilde{H}^a_T(\tilde{\eta}, \tilde{\xi})$ and $\widetilde{F}^a_T(\tilde{\theta}, \tilde{\xi}, \epsilon)$ are one-step consistent with $\widetilde{G}^e_T(k, \tilde{\theta}, \tilde{\eta}, \tilde{\xi})$, $\widetilde{H}^e_T(\tilde{\eta}, \tilde{\xi})$ and $\widetilde{F}^e_T(\tilde{\theta}, \tilde{\xi}, \epsilon)$. □

Next the main result states the conditions under which the approximate discrete-time model (19a), (19b) and (20) of the continuous-time ES controller (5a), (5b) and (6) is a valid discrete-time controller for the continuous-time plant (1) and preserves the stability property of the continuous-time controller under sampling.

Theorem 1. Suppose that Assumptions 1 and 2 hold. Let Δ come from Assumption 1 and $\widehat{\nu}$ be given. Then, for any $\widehat{\nu} > 0$ there exist ϵ^* such that for any fixed $\epsilon \in (0, \epsilon^*)$ there exists $\widehat{T}$ such that for all $T \in (0, \widehat{T})$, the following holds for the approximate discrete-time closed-loop system (19a), (19b) and (20):

$$|\tilde{\theta}^a(k)| \leq \beta_4(|(\tilde{\theta}(k_0), \tilde{\eta}(k_0), \tilde{\xi}(k_0)|, (k-k_0)T) + \widehat{\nu}, \qquad (21)$$

$$|\tilde{\eta}^a(k)| \leq \beta_5(|(\tilde{\eta}(k_0), \tilde{\xi}(k_0)|, (k-k_0)T) + \widehat{\nu}, \qquad (22)$$

$$|\tilde{\xi}^a(k)| \leq \beta_6\big(|\tilde{\xi}(k_0)|, \epsilon(k-k_0)T\big) + \widehat{\nu}, \qquad (23)$$

for all $|(\tilde{\theta}(k_0), \tilde{\eta}(k_0), \tilde{\xi}(k_0))| \leq \Delta$ and all $k \geq 0$. □

Sketch of Proof. The proof is omitted since it follows the approach used in Laila et al. (2002). □

The tuning procedure according to Theorem 1 is as follows. For any desired accuracy of the approximate discrete-time closed-loop system (19a), (19b) and (20) characterized by $\widehat{\nu}$, first the controller tuning parameters ϵ is adjusted to deliver appropriate convergence of the continuous-time scheme. Then the sample period T should be tuned so that (21)-(23) hold.

3.2 A particular discretization method

Here, the emulation method is applied to the parameter estimator (12a), (12b) and optimization algorithm (16) using the second order Runge-Kutta method. The obtained approximate discrete-time model in coordinates $\tilde{\theta} = \hat{\theta} - \theta$, $\widetilde{P} = P - P^*$ and $\tilde{\xi} = \xi - \xi^*$ is:

$$\begin{aligned}\tilde{\theta}(k+1) &= \tilde{\theta}(k) + \frac{1}{2}T\widetilde{G}(\tilde{\theta}(k), \widetilde{P}(k), \tilde{\xi}(k)) \\ &\quad + \frac{1}{2}T\widetilde{G}\left(\tilde{\theta}(k) + T\widetilde{G}(\tilde{\theta}(k), \widetilde{P}(k), \tilde{\xi}(k)), \widetilde{P}(k), \tilde{\xi}\right) \\ &= \widetilde{G}_T^a(\tilde{\theta}(k), \widetilde{P}(k), \tilde{\xi}(k)) \qquad (24a)\\ \widetilde{P}(k+1) &= \widetilde{P}(k) + \frac{1}{2}T\widetilde{H}(\widetilde{P}(k), \tilde{\xi}(k)) \\ &\quad + \frac{1}{2}T\widetilde{H}\left(\widetilde{P}(k) + T\widetilde{H}(\widetilde{P}(k), \tilde{\xi}(k)), \tilde{\xi}\right) \\ &= \widetilde{H}_T^a(\widetilde{P}(k), \tilde{\xi}(k)) \qquad (24b)\\ \tilde{\xi}(k+1) &= \tilde{\xi}(k) + \frac{1}{2}T\epsilon\widetilde{F}(\tilde{\theta}(k), \tilde{\xi}(k)) \\ &\quad + \frac{1}{2}T\epsilon\widetilde{F}\left(\tilde{\theta}, \tilde{\xi}(k) + T\epsilon\widetilde{F}(\tilde{\theta}(k), \tilde{\xi}(k))\right) \\ &= \widetilde{F}_T^a(\tilde{\theta}(k), \tilde{\xi}(k), \epsilon) \qquad (25)\end{aligned}$$

In order to verify Assumption 2 for this model a parameterized model of the plant is required which is investigated in the next section.

4. ES CONTROLLER DESIGN FOR THE SPARK ADVANCE OPTIMIZATION

In this section, using some experimental tests, it is shown that the composition of natural gases affect the MBT spark advance. Then, based on the obtained data a parameterized model of the plant is presented. Having the structure of the static plant, the discrete-time grey-box ES controller is designed for online optimization of the spark advance as fuel composition is varying.

4.1 The Effect of fuel composition variation on the MBT spark advance

The experiments are carried out in a six cylinder, 4L Ford Falcon BF MY2006 engine converted for CNG and connected to an eddy current type dynamometer. The fuel composition of two test gases are presented in Table 1. These compositions were chosen to represent extreme laminar flame speeds and consequently the spark advance, see Oostendorp and Levinsky (1990) for more details.

Open loop tests were performed at the engine operating condition of 1500rpm, 140Nm, and air/fuel ratio of 1. In these tests, for each gas composition, the brake torque is measured for different spark advances. Fig. 4 shows the test results. Two curves are obtained by fitting quadratic functions to the points near optimum values for each fuel composition.

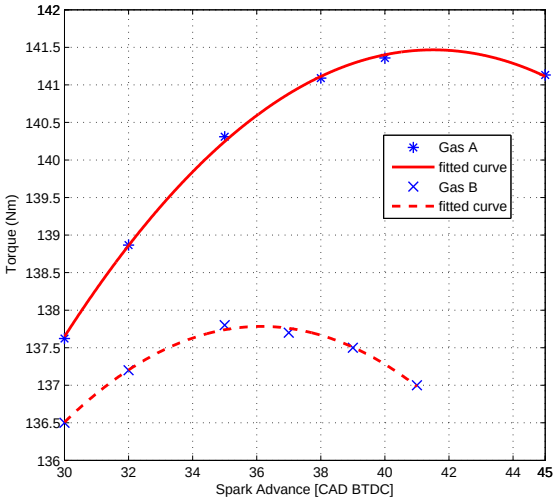

Fig. 4. Steady-state mapping between the spark advance and brake torque for Gas A (solid line) and Gas B (dashed line) - CAD BTDC means Crank Angle Degrees Before Top-Dead Center

Table 1. Composition of test gas fuels

	Gas A	Gas B
Methane	80	100
Ethane	2	0
Propane	0.5	0
Carbon Dioxide	9	0
Nitrogen	8.5	0

The results of the experiments were expected as the spark timing for Gas A need to advance because the inert gases retards the development of the flame. These results are similar to those observed in the study by Kim et al. (2009).

As depicted in Fig. 4, when the spark advance in fixed at MBT for Gas B, there is about 1% reduction in the brake torque of Gas A and vice versa.

4.2 Plant description

In order to apply the grey-box ES controller to adjust the spark advance, a parameterized model of the mapping between the spark advance and the brake torque is required. In Fig. 4 it is shown that this parameterized model is well represented by a quadratic function; i.e.:

$$\begin{aligned}\tau &= a\alpha_{sa}^2 + b\alpha_{sa} + c \\ &= h(\theta, \alpha_{sa}) \qquad (26)\end{aligned}$$

where τ is the engine brake torque, α_{sa} is the spark advance, $\theta = [a\ b\ c]^T$ is the unknown parameter vector and

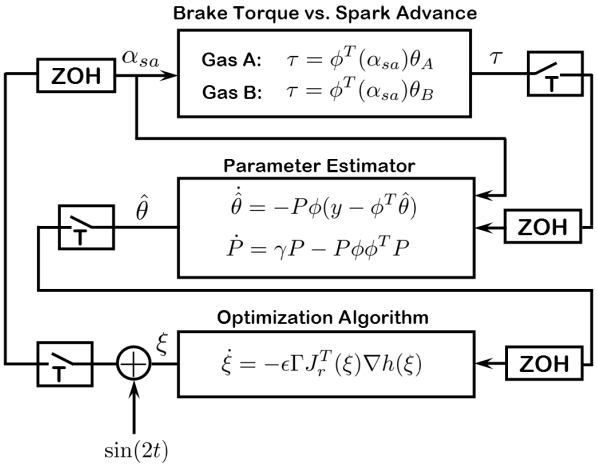

Fig. 5. Spark advance optimization block diagram for engines with varying fuel composition

a, b, c are unknown, nominally constant parameters for a given fuel composition. By introducing $\phi = [\alpha_{sa}^2 \;\; \alpha_{sa} \;\; 1]^T$, (26) can be written in the following compact form:

$$\tau = \phi^T(\alpha_{sa})\theta \tag{27}$$

Two curves in Fig. 4 correspond to two set of values for $\theta^T = [a \quad b \quad c]$ as $\theta_A^T = [-0.02886 \quad 2.396 \quad 91.75]$ and $\theta_B^T = [-0.0252 \quad 1.844 \quad 104]$. These set of parameters, θ_A and θ_B, are obtained via fitting quadratic curves to the mappings of Fig. 4 near optimum point which correspond to the Gas A and Gas B, respectively. Note that we do not have *a priori* knowledge neither about true values of parameters nor extremum values of the plant. The purpose of grey-box ES controller is to manipulate α_{sa} to optimize τ which is explained in the following subsection.

4.3 Discrete-time ES controller

Since the parameterized model of the plant is obtained in the previous subsection, now assumptions of Theorem 1 can be verified. First, Assumption 1 is verified for (12a), (12b) and (16). The vector $\phi(\alpha_{sa})$ in (27) satisfies condition (13) with dither signal $d(t) = \sin(2t)$. In addition, the Jacobian matrix $J_r(\hat{\theta}, \xi)$ in (15) for the function h in (26) is equal to $2a$. Since $a \neq 0$, so J_r is invertible. Therefore, Assumption 1 holds for (12a), (12b) and (16). Also, Assumption 2 holds for (24a), (24b) and (25) since regarding Definition 1:

- $\widetilde{G}_T^a$ and $\widetilde{H}_T^a$ are one-step consistent with $\widetilde{G}_T^{Euler}$ and $\widetilde{H}_T^{Euler}$ with $\rho(s) = s$ and $\widetilde{F}_T^a$ is one-step consistent with $\widetilde{F}_T^{Euler}$ with $\rho(s) = 4s + s^2 + \frac{1}{4}s^3$,
- $\widetilde{G}$, $\widetilde{H}$ and $\widetilde{F}$ are upper bounded and derivatives of $\widetilde{G}$ w.r.t $\tilde{\theta}$, $\widetilde{H}$ w.r.t $\widetilde{P}$ and $\widetilde{F}$ w.r.t $\tilde{\xi}$ are bounded so there exists a γ for each one.

Therefore, all assumptions of Theorem 1 hold and it can be concluded that by tuning the parameters ϵ and T, the approximate discrete-time closed-loop system (24a), (24b) and (25) has the properties (21), (22) and (23). Fig. 5 shows the spark advance optimization scheme using particular parameter estimator and optimization algorithm described above.

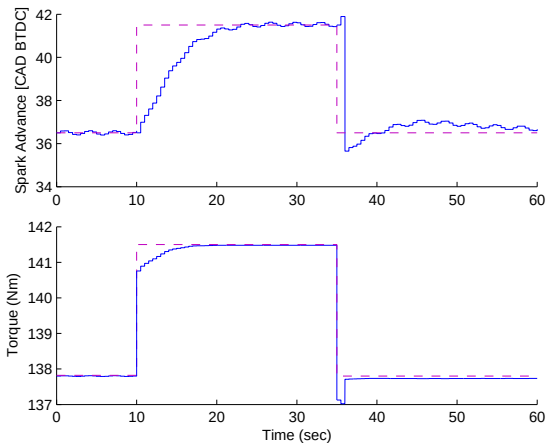

Fig. 6. Grey-box ES controller results for the no-noise case - Dashed lines shows the optimum values

5. SIMULATION RESULTS

In this section, the designed ES controller is applied to the static plant models of Fig. 4 in order to find the MBT spark advance as fuel composition varies from Gas A to Gas B and vice versa. For this purpose, it is assumed that initially the engine is calibrated for Gas B, therefore, the spark advance is initialized from $\alpha^*_{sa(GasB)} = \xi(0) = 36$ CAD BTDC which is the MBT spark spark advance of Gas B and corresponds to $\tau^*_{(GasB)} = 137.8Nm$, see Fig. 4. As a result, the controller should drive the spark advance to MBT spark advance of Gas A at $\alpha^*_{sa(GasA)} = 42$ CAD BTDC which corresponds to $\tau^*_{(GasA)} = 141.5Nm$ and then should converge to $\alpha^*_{sa(GasB)}$ again. The unknown parameters are initialized at $\hat{\theta}(0) = \theta_B = [-0.0252 \quad 1.844 \quad 104]^T$ and the sample time is $T = 0.5sec$. In the estimation algorithm (11a) and (11b), the covariance matrix is initialized at $P(0) = I_{3\times3}$ and $\gamma = 0.9$.

The simulation results are divided into two subsections. In the first subsection, it is assumed that there is no noise in the torque measurements. In the second subsection, a white noise signal is added on the output of plant to mimic the real engine measurements of the brake torque.

5.1 Convergence characteristics of the ES controller in absence of measurement noise

Fig. 6 shows the spark advance and the corresponding value of the brake torque. As mentioned earlier, initially (first $10sec$) the engine calibrated for the Gas B, therefore spark advance is in $\alpha^*_{sa(GasB)} = \xi(0) = 36$. Then, at $t = 10sec$ the fuel composition changes to Gas A. So the discrete-time grey-box ES controller achieves the values of 42 CAD BTDC for spark advance and holds that value until the fuel composition changes again at $t = 35sec$. Then, it converges to the MBT spark advance of Gas B again at 36 CAD BTDC and holds that value, with minor oscillations around the optimum point which are caused by the dither signal. The dither signal used here is the sinusoidal signal $d(t) = 0.1\sin(2t)$.

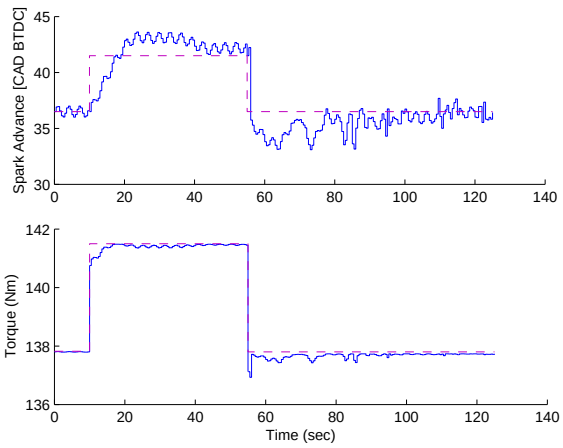

Fig. 7. Grey-box ES controller results in the presence of measurement noise - Dashed lines show the optimum values

5.2 The grey-box ES controller behavior in presence of measurement noise

From practical standpoint, due to the cyclic variability, the indicated mean effective pressure (IMEP) is varying and consequently the brake torque. The coefficient of variation of IMEP is typically used to quantify the cycle-to-cycle variation, defined as the standard deviation of IMEP divided by the mean IMEP and it is usually in percent. Based on the experimental tests, for both Gas A and Gas B, the coefficient of variation of IMEP was about 0.7% in the region of optimum points. Therefore, based on obtained data in experimental tests a zero-mean white noise with variance of 1 is added to the output torque of the plant.

All initial conditions are same as the previous subsection. The only parameter tuned for this case is the amplitude of the dither signal which is changed from 0.1 to 0.5 so $d(t) = 0.5\sin(2t)$. Fig. 7 shows that the grey-box ES controller can cope with the variation in fuel composition and measurement noise due to the cyclic variability, so that the spark advance is in its optimum value. As depicted in Fig. 7 after convergence to optimum spark advance it is still oscillating around the optimum value due to the dither signal required for the parameter estimation. However, this oscillation does not affect the brake torque too much.

5.3 Performance comparison of different grey-box schemes

As mentioned in Introduction, a large class of estimators can be combined with a large class of optimizers in the proposed grey-box ES framework. In this section, closed-loop performance of different combinations of parameter estimators and optimization algorithms are investigated. To this end, first a fair assessment criterion should be employed. The criterion used here is based upon a modified version of the average power loss (APL) proposed by Scotson and Wellstead (1990). In this criterion, the mean deviation of the actual engine brake torque, τ, from its achievable maximum, τ^* is accumulated over an operating span. Thus, the average power loss over $[k_0T, kT]$ is defined as

$$APL(k_0,k) = \frac{1}{(k-k_0)}\sum_{i=k_0}^{k}[\tau^* - \tau(i)] \qquad (28)$$

Typically, the APL is normalized by expressing it as a percentage of the maximum achievable performance, τ^*; therefore, the values in Table 2 are in terms of $\%APL$, i.e.:

$$\%APL(k_0,k) = \frac{APL(k_0,k)}{\tau^*} \times 100, \qquad (29)$$

where τ^* is the maximum torque in each fuel composition. The value of τ^* changes as the fuel composition changes.

Table 2. Performance comparison of different combination of estimators and optimizers regarding %APL

	OA1	OA2	OA3	OA4	OA5	OA6
EA1	0.105	0.099	0.096	0.095	0.084	0.083
EA2	0.071	0.088	0.083	0.081	0.082	0.084
EA3	0.079	0.077	0.074	0.072	0.076	0.077
EA4	0.081	0.072	***0.070***	0.073	0.071	0.072
Without ES	0.53					

Table 2 shows that some combinations of optimization algorithms (OA) and estimation algorithms (EA) lead to better closed-loop behavior under some conditions. The %APL of the particular estimator and optimizer used in the previous section is highlighted in Table 2 which is 0.070. Comparing the performance of this combination with the worst combination (EA1 and OA1), it shows about %30 improvement. In addition, comparing it with the case that there is no ES controller, the result is about 7 times better. Therefore, it is worthwhile to use grey-box ES control and to try different combinations to find the ES algorithm that has the best performance since different combinations are suited for different type of problems.

6. CONCLUSIONS AND FUTURE WORKS

This contribution showed the feasibility of applying grey-box extremum seeking framework in practical engineering problems. In particular, the grey-box ES framework is utilized to design a controller for online optimization of spark advance in automotive engine. This is primarily of interest in alternative fueled engines due to the varying composition of the fuel. The simulation results showed that the grey-box ES controller is robust enough to cope with this situation. This paper also demonstrated the flexibility of the framework by using different parameter estimators and optimization algorithms.

The grey-box ES controller presented in this paper will be used in experiments on a CNG fueled engine in future. The aim of these experiments is to adjust the spark advance online as the fuel composition changes.

REFERENCES

Absil, P. A. and Kurdyka, K. On the stable equilibrium points of gradient systems. *Systems & Control Letters*, Vol. 55, pp. 573-77, 2006.

Baras, J. S., Bensoussan A. and James M. R. Dynamic Observer as Asymptotic Limits of Recursive Filters: Special Cases. *J. Appl. Math.*, Vol. 5, No. 48, pp. 1147-58, 1988.

Bhaya, A. and Kaszkurewicz, E. Control perspectives on numerical algorithms and matrix problems. *siam publication*, 2006.

Egardt, B. and Larsson, S., On a Parameter Adaptive Extremum Controller. *IEEE Control and Decision Conference*, Seville, Spain, December 12-15, 2005.

Eriksson, L. Spark advance for optimal efficiency. *SAE Paper*, 1999-01-0548, 1999.

Ioannou, P. and Fidan, B. Adaptive Control Tutorial. *siam Publications*, 2006.

Keynejad, F. Improving Engine Cold Start Performance through Optimal Control Strategies. *PhD Thesis*, Dept. of Mech. Eng., Univesity of Melbourne, Melbourne, 2009.

Killingsworth, N.J., Aceves, S.M., Flowers, D.L., Espinosa-Loza, F. and Krstic, M. HCCI Engine Combustion-Timing Control: Optimizing Gains and Fuel Consumption Via Extremum Seeking. *IEEE Transactions on Control Sys. Tech.*, vol. 17, No. 6, pp. 1350-61, 2009.

Kim, K., Kim, H., Kim, B., Lee, K. and Lee, K. Effect of Natural Gas Composition on the Performance of a CNG Engine. *Oil and Gas Science and Technology Rev. IFP*, Vol. 64, No. 2, pp. 199-206, 2009.

Laila, D. S., Nešić, D. and Teel, A. Open and closed loop dissipation inequalities under sampling and controller emulation. *European Journal of Control*, Vol. 8, No. 12, pp. 119-125, 2002.

Ly, H. Effects of Natural Gas Composition Variations on the Operation Performance and Exhaust Emissions of Natural Gas-Powered Vehicles. *Proc. NGV Conf.*, 2002.

Min, B., Bang, K. and Kim, H. Effects of Gas Composition on the Performance and Hydrocarbon Emissions for CNG Engines. *SAE paper*, No. 981918, 1998.

Nešić, D. Extremum seeking control: convergence analysis. *Europ. J. Contr.*, vol. 15, No. 3-4, pp. 331-347, 2009.

Nešić, D., Mohammadi, A. and Manzie, C. A Framework for Extremum Seeking Control of Systems with Parameter Uncertainties. *IEEE Transaction on Automatic Control*, to appear in Feb. 2013, DOI: 10.1109/TAC.2012.2215270.

Oostendorp, D. L. and Levinsky, H. B. The effects of fuel and non-fuel gases on the laminar burning velocity of methane-air flames. *Journal of the Institute of Energy*, vol. 63, pp. 160-166, 1990.

Pierre, D. A. and Pierre, J. W. Digital controller design - Alternative emulation approaches. *ISA Transactions*, vol. 34, pp. 219-28, 1995.

Popović, D., Janković, M., Magner, S. and Teel, A. R. Extremum Seeking Methods for Optimization of Variable Cam Timimg Engine Operation. *IEEE Trans. on Contr. Sys. Tech.*, vol. 14, No. 3, pp. 398-407, 2006.

Scotson, P. and Wellstead, P. E. Self-tuning optimization of spark ignition automotive engines. *IEEE Control Sys. Mag.*, vol. 3, no. 10, pp. 94-101, Apr. 1990.

Tanabe, K. Global analysis of continuous analogues of the Levenberg-Marquardt and Newton-Raphson methods for solving nonlinear equations. *Annals of the Institute of Statistical Mathematics*, Vol. 37, No. 1, pp. 189-203, 1985.

Zarrop, M. B. and Romments M. J. J. J. Convergence of a multi-input adaptive extremum controller. *IEE Proceedings Part D Control Theory and Applications*, vol. 140, no. 2, pp. 65-69, Apr. 1993.

Zhang, L. H., Kelley, C. T., Liao, L. Z. A continuous Newton-type method for unconstrained optimization. *Pacific J. of Optimization*, Vol. 4, No. 2, pp. 259-77, 2008.